

TECHNICAL NOTE

D-361

FREE-FLIGHT MEASUREMENTS OF THE
TRANSONIC DRAG CHARACTERISTICS OF LOW-FINENESS-RATIO
CYLINDERS INCLUDING STABILIZING PLATES AND FLARES
AND VARYING NOSE BLUNTNESS

By Joseph H. Judd and Gerard E. Woodbury

Langley Research Center
Langley Field, Va.

(NASA-TN-D-361) FREE-FLIGHT MEASUREMENTS OF
THE TRANSONIC DRAG CHARACTERISTICS OF
LOW-FINENESS-RATIO CYLINDERS INCLUDING
STABILIZING PLATES AND FLARES AND VARYING
NOSE BLUNTNESS (NASA. Langley Research

N89-71137

Unclas
00/02 0198968

NATIONAL AERONAUTICS AND SPACE ADMINISTRATION

WASHINGTON

May 1960

G

NATIONAL AERONAUTICS AND SPACE ADMINISTRATION

TECHNICAL NOTE D-361

FREE-FLIGHT MEASUREMENTS OF THE
TRANSONIC DRAG CHARACTERISTICS OF LOW-FINENESS-RATIO
CYLINDERS INCLUDING STABILIZING PLATES AND FLARES
AND VARYING NOSE BLUNTNESS

L
8
5
7

By Joseph H. Judd and Gerard E. Woodbury

SUMMARY

Various blunt-nose configurations of low fineness ratio were tested in free flight from Reynolds numbers per foot of 4.0×10^6 to 8.3×10^6 and from Mach numbers of 0.6 to 1.2. The basic configuration was a right circular cylinder of a fineness ratio of 2.0. A single stabilizing plate at the front and at the rear was tested and also a 16.5° conical flare. Various nose radii were tested along with 16.5° truncated-cone nose fairings.

All stabilizing devices increased the drag coefficient of the right circular cylinder inasmuch as the projected frontal area was doubled. The conical-flare model, however, only had 30 percent more drag than the cylinder. The truncated-cone nose fairings were more effective than the circular-arc nose fairings in reducing drag coefficient at the test Reynolds numbers and Mach numbers.

INTRODUCTION

Until recent years, the drag studies of aeronautical shapes have been mainly concerned with relatively slender, smooth shapes as exemplified by the models of reference 1. However, with the advent of ballistic missiles and satellite flight, the short high-drag body has become important. The short cylinder is a relatively efficient container, and the blunt high-drag body has been shown (ref. 2) to absorb less total heat by convection while decelerating from hypersonic speeds than the low-drag body. The investigation reported herein was undertaken by the Applied Materials and Physics Division of the Langley Research Center to measure the transonic drag of various blunt-nose bodies of revolution of low fineness ratio.

The initial configuration selected for testing was a right circular cylinder of fineness ratio of 2.0. Front and rear stabilizing plates and a stabilizing flare were added to the cylinder. Also, circular-arc and truncated-cone nose fairings were added to the flare-stabilized cylinder. Free-flight tests were made at the NASA Wallops Station using the helium-gun facility. Drag data were obtained from Mach numbers 0.6 to 1.2 and Reynolds numbers per foot from 4.0×10^6 to 8.3×10^6 .

SYMBOLS

A	cylinder cross-sectional area
A_F	nose flat area
A_T	maximum cross-sectional area
C_D	drag coefficient, based on A
D_b	cylinder diameter
M	free-stream Mach number
R	Reynolds number per foot
x_{cg}	model center of gravity measured from the nose

MODELS, TESTS, AND ANALYSIS

Drawings of the test models are presented in figure 1. The basic model tested was a right circular cylinder of fineness ratio of 2.0. A stabilizing plate of 1.43 cylinder diameters was attached to the front of one model, and to the rear of another model. In addition, a 16.5° conical-flare model was tested. Four models with circular-arc nose fairings and conical flares were also tested. Two 16.5° truncated-cone nose fairings with the conical flare were tested. Table I presents the flat- and total-area ratios together with the center-of-gravity locations for the test configurations. Two models of each configuration were flown with the exception of model 5. Models 5 and 5(a) differed in cylinder length by approximately 5 percent (1/16 inch). The forward section of each model was machined from sintered tungsten and the after section from magnesium. The two

sections were assembled by steel pins. Each model had a root-mean-square roughness of 125 microinches.

The models were propelled to supersonic speeds from a helium gun at the NASA Wallops Station. The helium-gun test technique and a description of the equipment used are presented in reference 3. The instrumentation used for these tests consisted of ground tracking radar, CW Doppler velocimeter, and rawinsonde. The drag data were obtained by the CW Doppler velocimeter technique described in reference 4. All velocities were corrected for the wind component obtained from the rawinsonde. The drag curves presented are mean curves of values obtained from the testing of two models of each configuration.

Although the models were ballasted to be statically stable, they have low damping rates due to their low fineness ratio and bluntness. Model oscillations due to disturbances as a result of ejection from the helium gun would induce oscillations about a low-lift trim angle or zero-lift trim that would be sustained through most of the test range. The resulting measured drag coefficients, as reduced from the CW Doppler velocimeter, represent average values of drag about zero lift or a low-lift trim. However, reference 5 shows that for the flat-nose configurations the variations of C_D with angle of attack are very small.

The Mach number measurements are accurate to ± 0.01 . The measured differences between drag measurements for each pair of models were within 0.1 over the test range.

RESULTS AND DISCUSSION

The Reynolds number per foot for the tests varied from 4.0×10^6 to 8.3×10^6 and from Mach numbers 0.6 to 1.2 as shown in figure 2. The variation of drag coefficient, based on cylinder diameter, with Mach number is presented in figure 3 for models 1 to 10.

A comparison of the drag coefficients of models 1 to 4 was made in figure 4. These models represent the cylinder with various methods of stabilization. All stabilizing devices gave the configurations higher drag coefficients than the cylinder since the projected frontal area was doubled. The addition of the 16.5° flare to the cylinder added approximately 30 percent drag. At a Mach number of 0.6 the cylinder with the stabilizing plate at the nose had only 2 percent more drag than the cylinder with the plate at the rear. At Mach numbers above 1.0, the configuration with the rear stabilizing plate had only 10 percent more drag than the flare stabilized cylinder.

The variation of total drag coefficients of the circular-arc nose-fairing configurations, models 5 to 8, with the ratio of nose flat area to cylinder area are presented in figure 5 for Mach numbers of 0.6, 0.9, and 1.1 and corresponding Reynolds numbers per foot of 4×10^6 , 6×10^6 , and 7×10^6 . The average values of drag coefficient for models 5 and 5a were used. The largest reduction in drag coefficient occurred at subsonic speeds where a reduction in total drag coefficient of about 50 percent was obtained from a flat-nose configuration, model 3 ($A_F/A = 1.00$), to a nearly hemispherical nose configuration, model 8 ($A_F/A = 0.04$). At transonic speeds a drag reduction of approximately 25 percent occurred from $A_F/A = 1.00$ to $A_F/A = 0.04$. Figure 6 presents the variation of total drag coefficient with nose flat area ratio to cylinder area ratio for the truncated-cone nose fairing. A reduction in total drag coefficient of about 37 percent was obtained from model 10 ($A_F/A = 0.30$) to the flat-nose configuration model 3 ($A_F/A = 1.00$) at Mach number 1.1. The reduction in total drag coefficient with nose flat area ratio was greater for the truncated-cone nose fairing than for the circular-arc nose fairings over the Reynolds number and Mach number range tested.

CONCLUDING REMARKS

Flight tests of a series of blunt-nose configurations of low fineness ratio were made from Reynolds numbers per foot of 4.0×10^6 to 8.3×10^6 and from Mach numbers of 0.6 to 1.2. Configurations consisted of a right circular cylinder with stabilizing plates and a 16.5° flare and various radii circular-arc and truncated-cone nose fairings.

All stabilizing devices increased the drag over that of the basic configuration which was a right circular cylinder of fineness ratio of 2.0. The 16.5° flare gave the smallest increase in the drag coefficient and averaged about 30 percent over the test range.

Truncated-cone nose fairings were more effective on the flare stabilized cylinder than the circular-arc nose fairings in reducing drag coefficients for the Reynolds number and Mach number ranges covered.


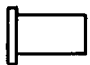
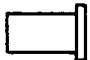






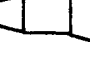
Langley Research Center,
National Aeronautics and Space Administration,
Langley Field, Va., January 15, 1960.

REFERENCES

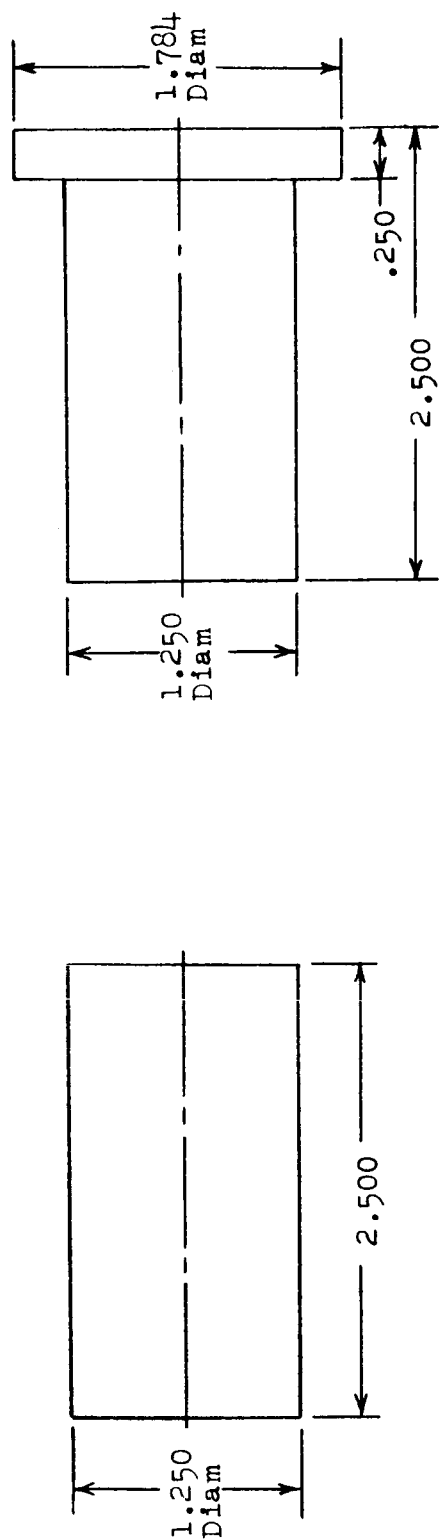
1. Stoney, William E., Jr.: Collection of Zero-Lift Drag Data on Bodies of Revolution From Free-Flight Investigations. NACA TN 4201, 1958.
2. Allen, H. Julian, and Eggers, A. J., Jr.: A Study of the Motion and Aerodynamic Heating of Ballistic Missiles Entering the Earth's Atmosphere at High Supersonic Speeds. NACA Rep. 1381, 1958. (Supersedes NACA TN 4047.)
3. Hall, James Rudyard: Comparison of Free-Flight Measurements of the Zero-Lift Drag Rise of Six Airplane Configurations and Their Equivalent Bodies of Revolution at Transonic Speeds. NACA RM L53J21a, 1954.
4. Wallskog, Harvey A., and Hart, Roger G.: Investigation of the Drag of Blunt-Nosed Bodies of Revolution in Free Flight at Mach Numbers From 0.6 to 2.3. NACA RM L53D14a, 1953.
5. Lichtenstein, Jacob H., Fisher, Lewis R., Scher, Stanley H., and Lawrence, George F.: Some Static, Oscillatory, and Free-Body Tests of Blunt Bodies at Low Subsonic Speeds. NASA MEMO 2-22-59L, 1959.

TABLE I

MODEL AREA RATIOS

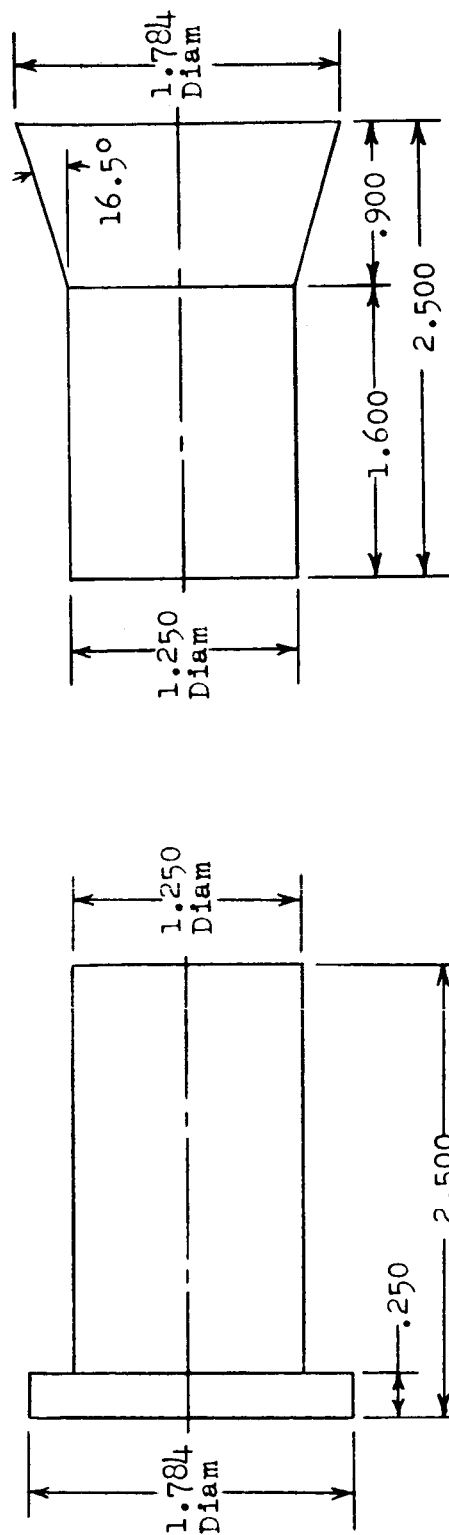
Model	A_F/A	A_T/A	A_F/A_T	x_{cg}/D_b	Shape
1	1.000	1.000	1.000	0.604	
2	2.039	2.039	1.000	.591	
3	1.000	2.039	.489	.620	
4	1.000	2.039	.489	.628	
5 and 5a	.640	2.039	.315	.629	
6	.360	2.039	.176	.678	
7	.160	2.039	.079	.744	
8	.040	2.039	.020	.808	
9	.416	2.039	.204	.800	
10	.300	2.039	.148	.910	

L
8
5
7



(a) Model 1.

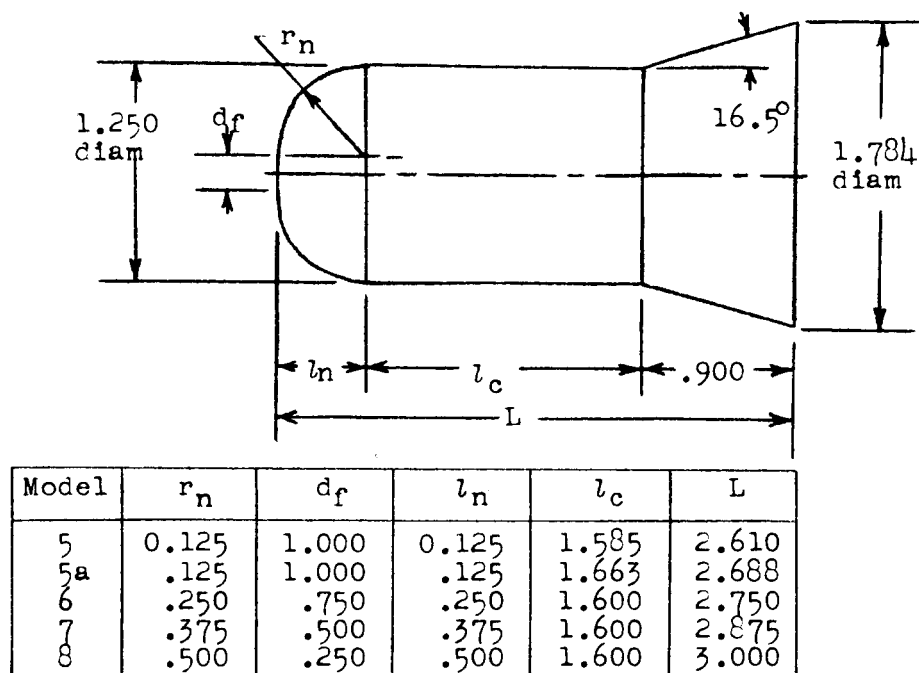
(c) Model 3.



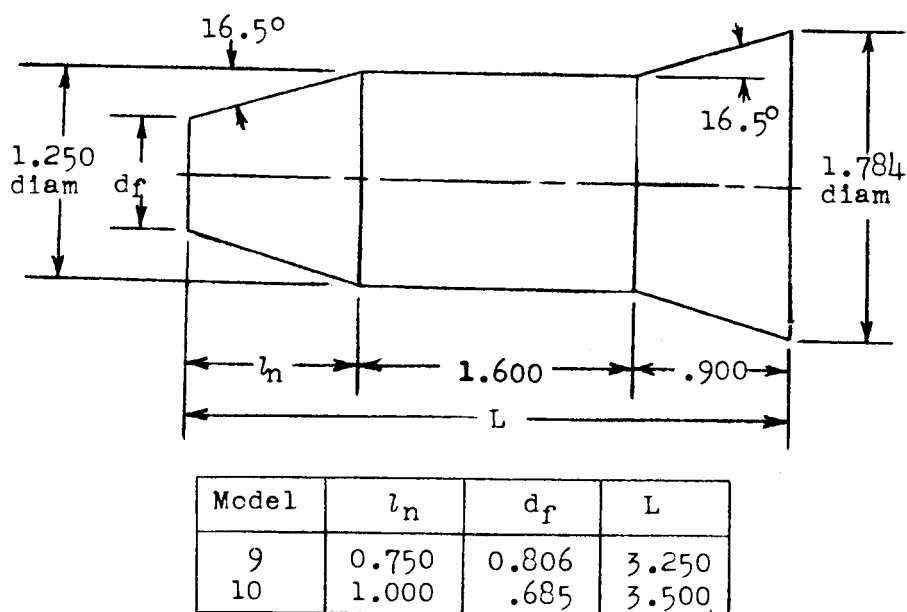
(b) Model 2.

(d) Model 4.

Figure 1.- Drawings of helium-gun models. All dimensions are in inches.



(e) Models 5 to 8.



(f) Models 9 and 10.

Figure 1.- Concluded.

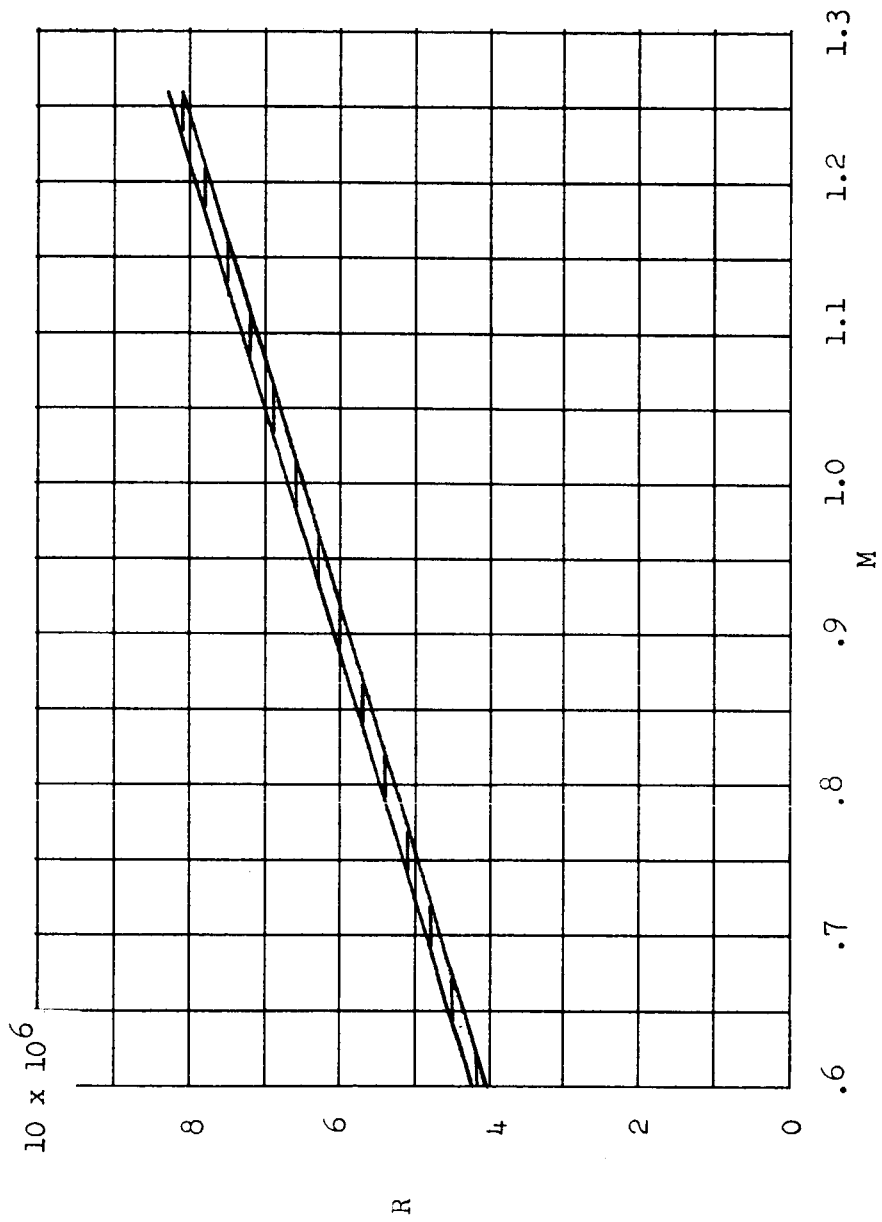
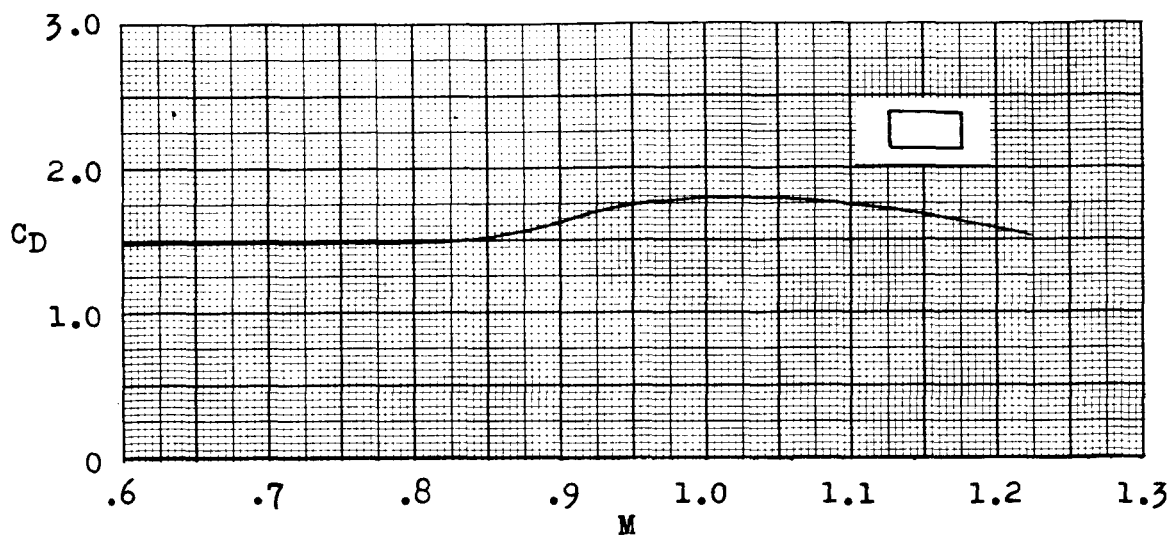
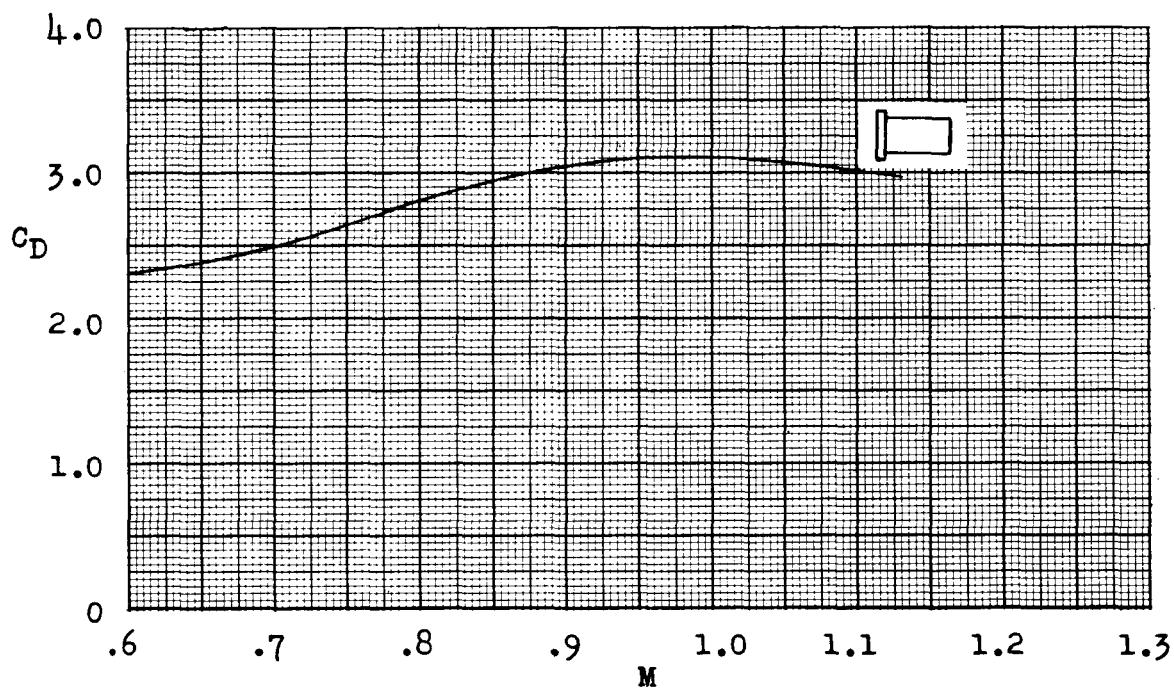


Figure 2.- Variation of Reynolds number per foot with Mach number.

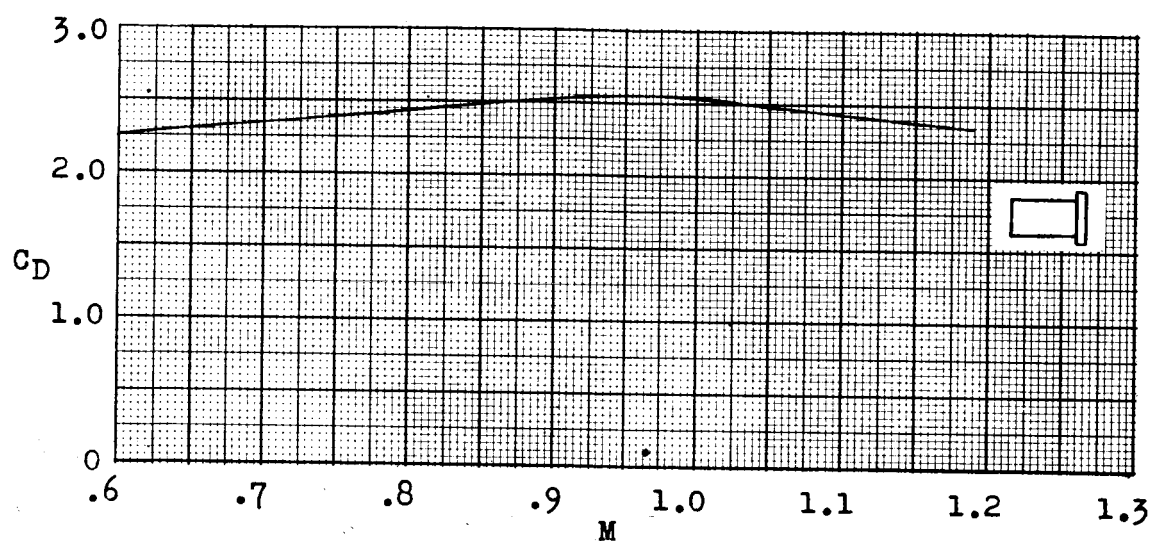


(a) Model 1.

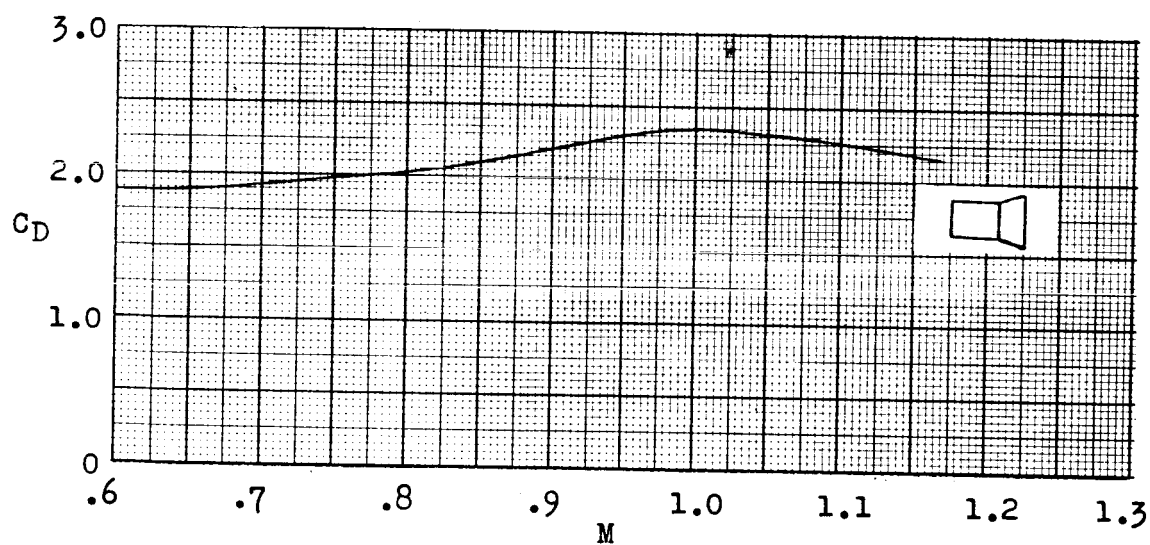


(b) Model 2.

Figure 3.- The variation of drag coefficient, based on cylinder diameter, with Mach number for the helium-gun models.

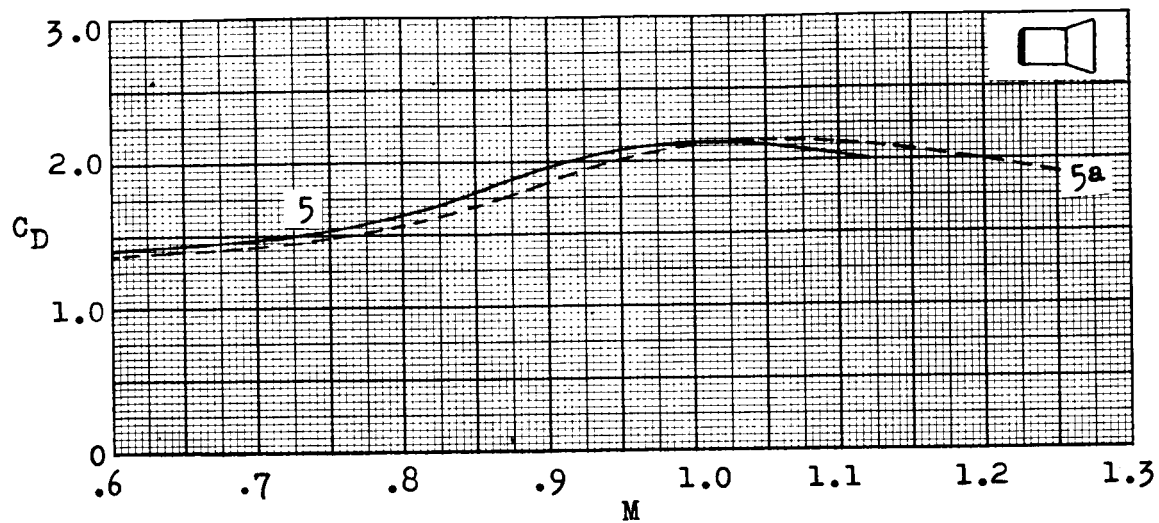


(c) Model 3.

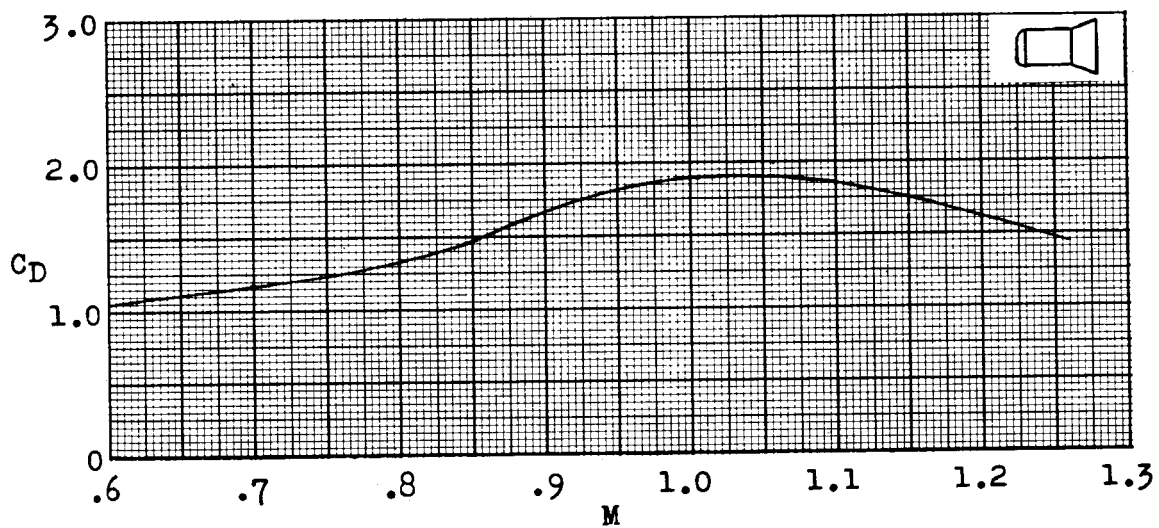


(d) Model 4.

Figure 3.- Continued.

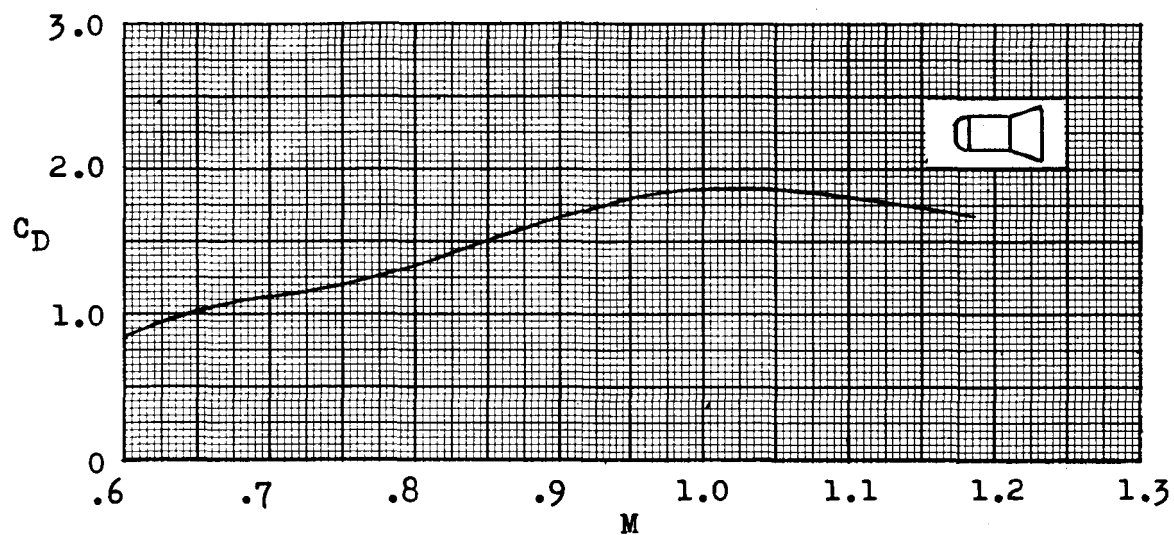


(e) Models 5 and 5a.

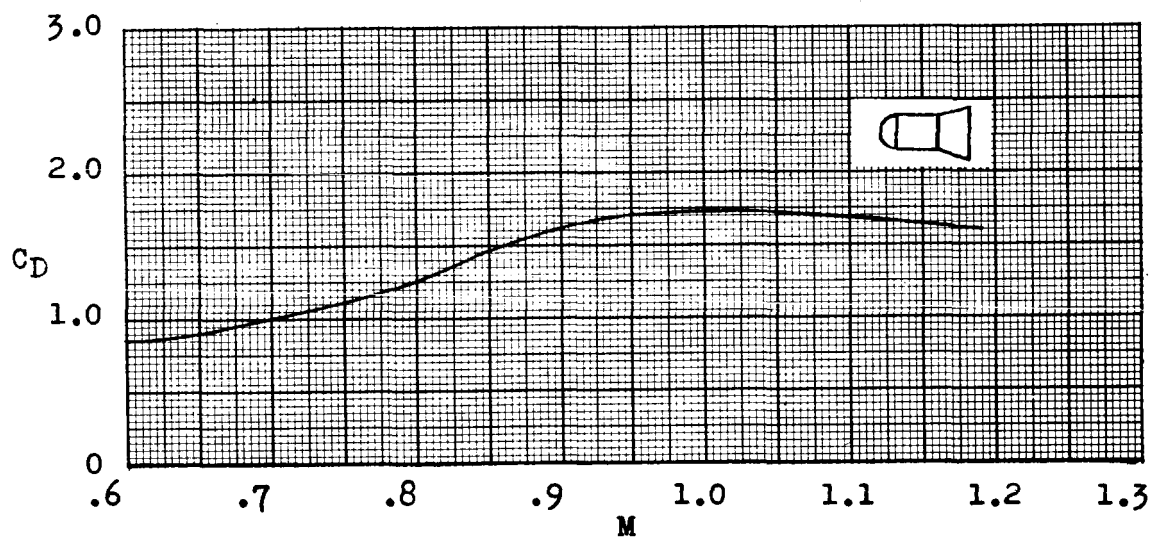


(f) Model 6.

Figure 3.- Continued.

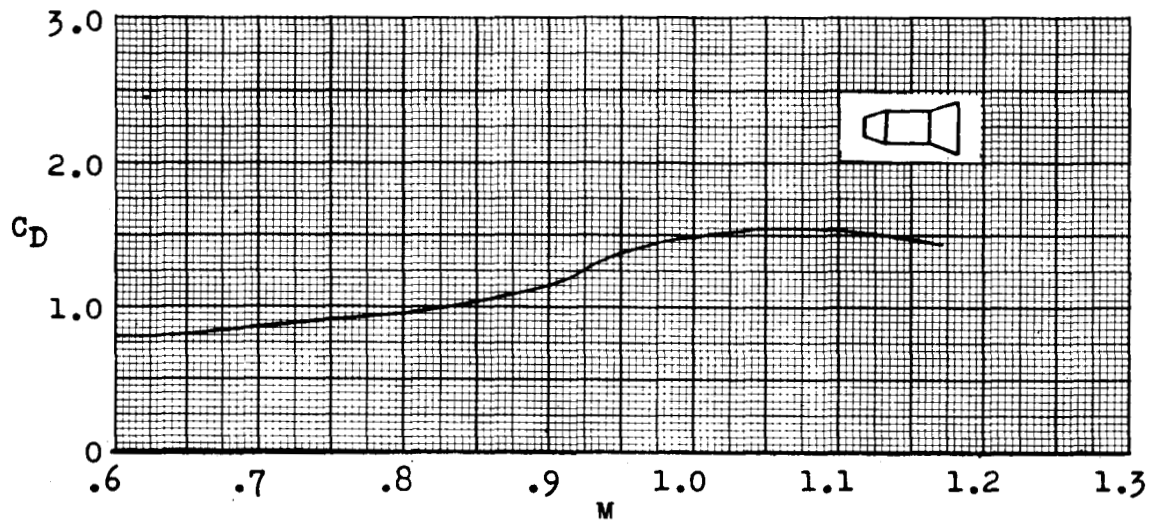


(g) Model 7.

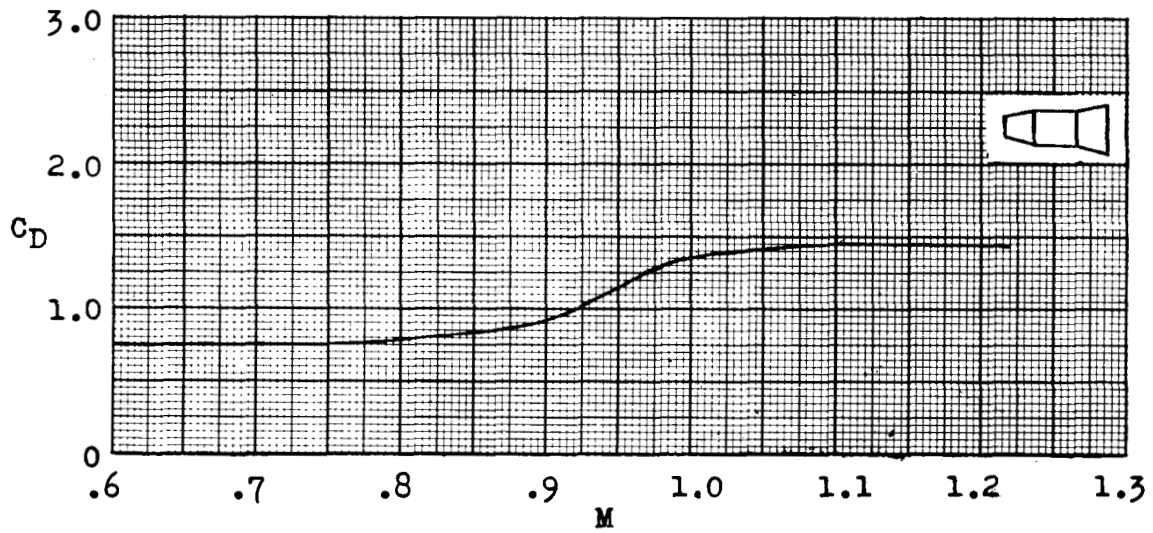


(h) Model 8.

Figure 3.- Continued.



(i) Model 9.



(j) Model 10.

Figure 3.- Concluded.

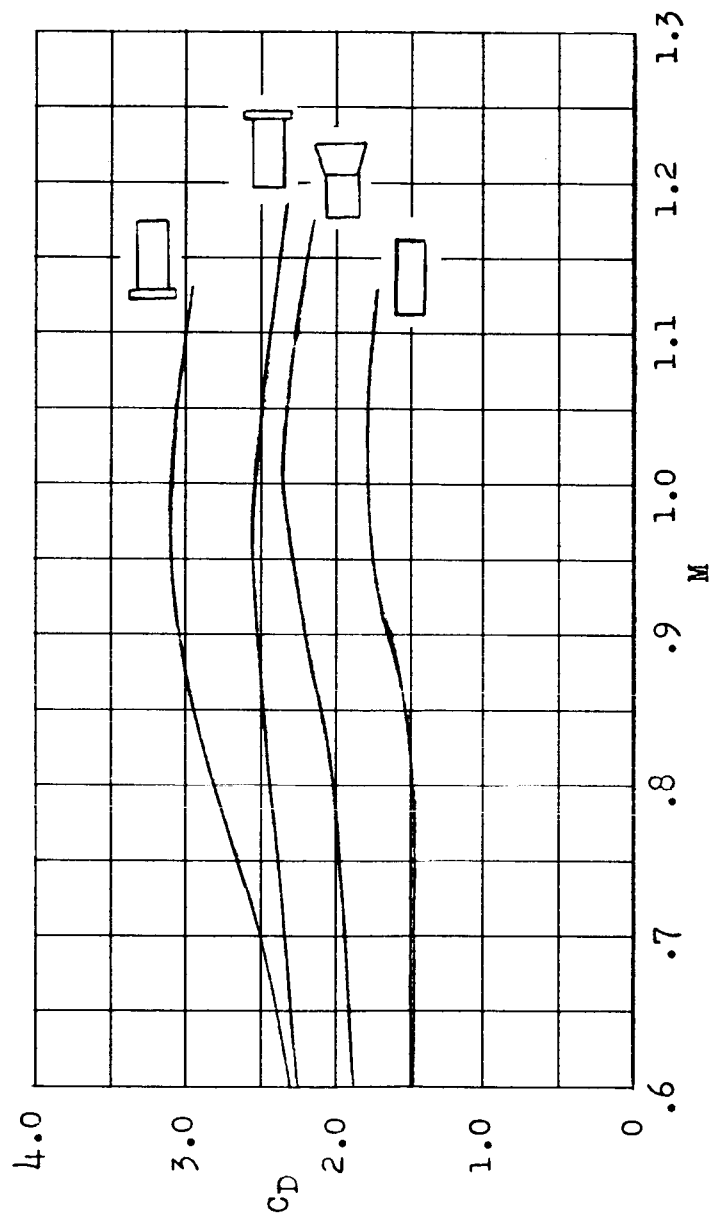


Figure 4.- Comparison of drag coefficients of right circular cylinders with various stabilizing devices.

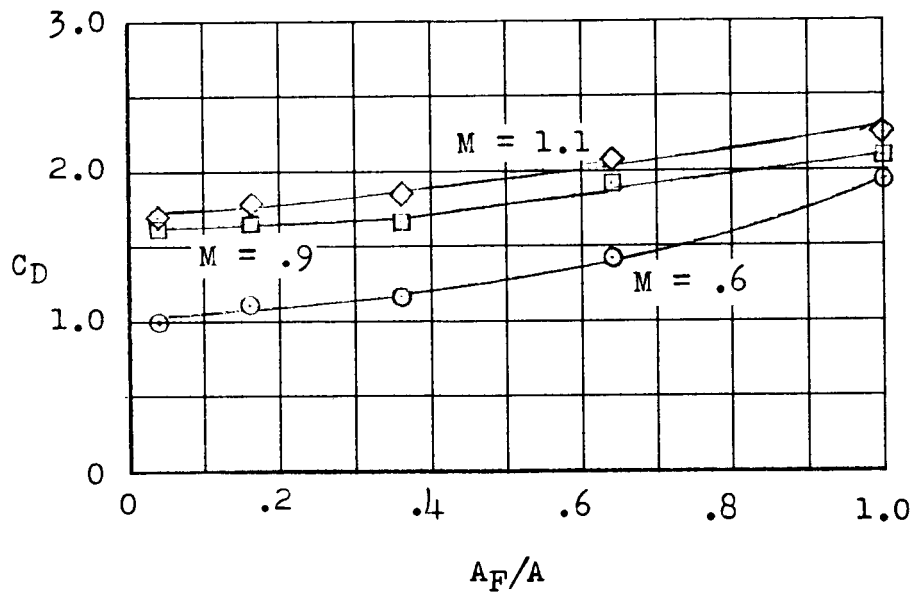


Figure 5.- Effect of circular-arc nose fairings on total drag coefficients.

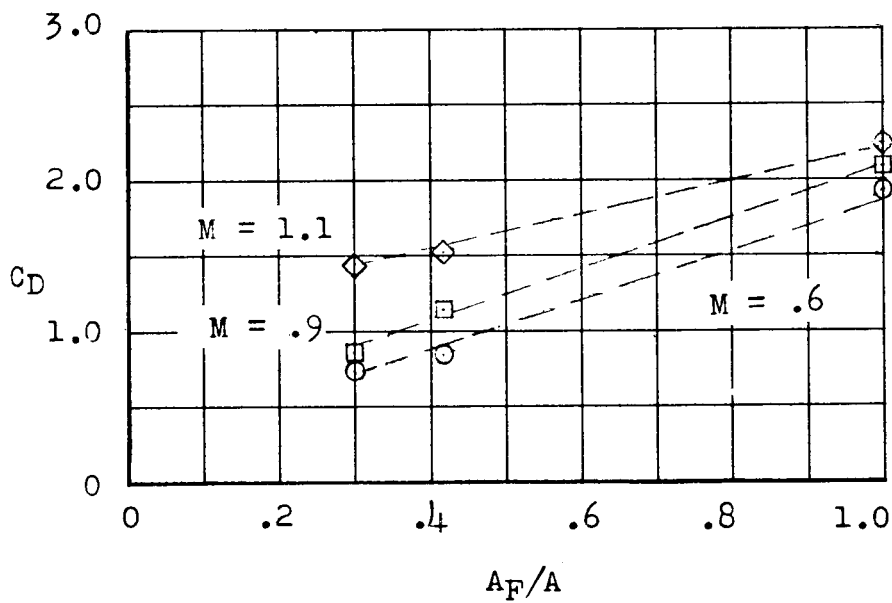


Figure 6.- Effect of truncated-cone nose fairings on total drag coefficients.